



HAL
open science

Why are cellular switches Boolean? General conditions for multistable genetic circuits

Javier Macía, Stefanie Widder, Ricard Solé

► To cite this version:

Javier Macía, Stefanie Widder, Ricard Solé. Why are cellular switches Boolean? General conditions for multistable genetic circuits. *Journal of Theoretical Biology*, 2009, 261 (1), pp.126. 10.1016/j.jtbi.2009.07.019 . hal-00559145

HAL Id: hal-00559145

<https://hal.science/hal-00559145>

Submitted on 25 Jan 2011

HAL is a multi-disciplinary open access archive for the deposit and dissemination of scientific research documents, whether they are published or not. The documents may come from teaching and research institutions in France or abroad, or from public or private research centers.

L'archive ouverte pluridisciplinaire **HAL**, est destinée au dépôt et à la diffusion de documents scientifiques de niveau recherche, publiés ou non, émanant des établissements d'enseignement et de recherche français ou étrangers, des laboratoires publics ou privés.

Author's Accepted Manuscript

Why are cellular switches Boolean? General conditions for multistable genetic circuits

Javier Macía, Stefanie Widder, Ricard Solé

PII: S0022-5193(09)00322-1
DOI: doi:10.1016/j.jtbi.2009.07.019
Reference: YJTBI5627

To appear in: *Journal of Theoretical Biology*

Received date: 13 January 2009
Revised date: 6 July 2009
Accepted date: 6 July 2009

Cite this article as: Javier Macía, Stefanie Widder and Ricard Solé, Why are cellular switches Boolean? General conditions for multistable genetic circuits, *Journal of Theoretical Biology*, doi:10.1016/j.jtbi.2009.07.019

This is a PDF file of an unedited manuscript that has been accepted for publication. As a service to our customers we are providing this early version of the manuscript. The manuscript will undergo copyediting, typesetting, and review of the resulting galley proof before it is published in its final citable form. Please note that during the production process errors may be discovered which could affect the content, and all legal disclaimers that apply to the journal pertain.



www.elsevier.com/locate/jtbi

Why are cellular switches Boolean?

General conditions for multistable genetic circuits

Javier Macía ^{a,1}, Stefanie Widder ^{a,*,1}, Ricard Solé^{a,b}

^a*Complex System Lab (ICREA-UPF), Barcelona Biomedical Research Park (PRBB-GRIB), Dr. Aiguader 88, 08003 Barcelona, Spain*

^b*Santa Fe Institute, 1399 Hyde Park Road, Santa Fe NM 87501, USA*

Abstract

The logic of cellular decision making is largely controlled by regulatory circuits defining molecular switches. Such switching elements allow to turn a graded input signal into an all-or-nothing output. Traditional studies have focused on this bistable picture of regulation, but higher-order scenarios involving tristable and tetrastable states are possible too. Are these multi-switches allowed in simple gene regulatory networks? Are they likely to be observed? If not, why not? In this paper we present the examination of this question by means of a simple but powerful geometric approach. We examine the relation between multistability, the degree of multimerization of the regulators and the role of autoloops within a deterministic setting, finding that N -stable circuits are possible, although their likelihood to occur rapidly decays with the order of the switch. Our work indicates that, despite two-component circuits are able to implement multistability, they are optimal for Boolean switches. The evolutionary implications are outlined.

Key words: tristability, multistability, minimal genetic circuit, nullclines

*To whom correspondence should be addressed. Email: stefanie.widder@upf.edu

¹The authors have contributed equally.

analysis

PACS: APS/123-QED

1. Introduction

Bistability is a dynamical phenomenon related to the core processes in biological systems. During the last decade numerous experimental and theoretical studies were devoted to analyze its formal properties and its natural occurrence (Hasty et al. (2001); Cherry and Adler (2000); Laurent and Kellershohn (1999); Novak and Tyson (2003); Widder et al. (2007)). Although it pervades many different biological processes, it is reasonable to assume that cellular decision-making is not only based on binary solutions. Actually, the complex nature of gene regulatory circuits allows them to display multiple alternative steady status (Boyer et al. (2005); Niwa et al. (2005); Zhou et al. (2007); Cinquin and Demongeot (2005); Cantor and Orkin (2001); Li (2002); Delbrück (1949)). In this context, bistability would be a limit case of bifurcations in low-dimensional dynamical systems. If N is the number of possible attractors of a given system, $N = 2$ would perhaps be likely to occur in low-dimensional networks. Examples of multiple stable solutions can be found in development, such as embryonic stem cell master regulators (Boyer et al. (2005); Niwa et al. (2005); Zhou et al. (2007)), hematopoietic lineage specification (Cinquin and Demongeot (2005); Cantor and Orkin (2001)) or epigenetic processes resulting in phenotypic differences (Li (2002); Delbrück (1949)). These processes account for multiple valid alternatives, for example in response to external conditions, crucially important for adaptive behaviour. Many of these systems have a two-component

circuit operating at the core of the decision-making process. This occurs with *Xenopus oocytes*, which convert a continuously variable concentration of the maturation-inducing hormone progesterone, into an all-or-none biological maturation response Ferrell and Machleder (1998). Stem cells on the other hand display a switch-like response, where the expression of the involved transcription factors (OCT4, SOX2, and NANOG) are stabilized by a bistable switch. When they are expressed and the switch is ON, the self-renewal genes are ON and the differentiation genes are OFF. The opposite holds when the switch is OFF (Chickarmane et al. (2006)). A third example is the cell-cycle regulation, which exhibits a temporally abrupt response of Cdc2 to non-degradable cyclin B (Pomerening et al. (2003)). The question here is: are two-component circuits compatible only with bistable ($N = 2$) patterns? Or are these circuits instead capable of multistable ($N > 2$) behaviour? (Kaufman and Thomas (1987); Ma and Wu (2007); Demongeot et al. (2000); Ozbudak et al. (2004); Tyson et al. (2003)). We can pose these problems in terms of general questions such as: Is the logic of cellular decisions Boolean? If it is, why is that?

Despite the question about the presence of multistability in two-component circuits has been previously addressed (Snoussi and Thomas (1993)), several questions remain open. Among them three seem particularly relevant: (a) How the degree of multimerization correlates with the potential multistability achievable, (b) how likely is the emergence of systems with $M > 2$ multistability, and (c) how the degree of multimerization determines the robustness of these minimal circuits are questions addressed in this work.

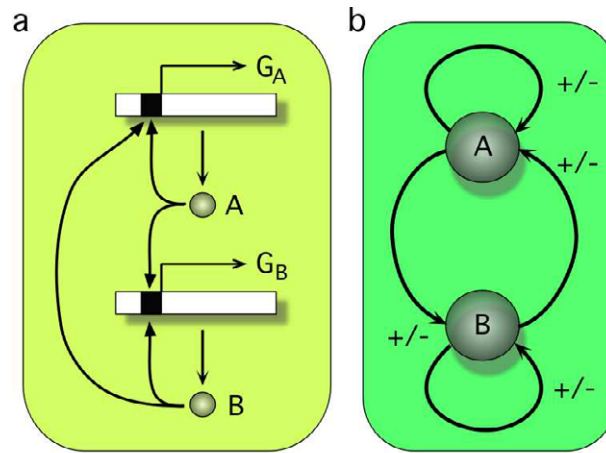


Figure 1: (a) A genetic circuit with multimeric autoloops and cross-regulation involving two genes (G_A , G_B) coding for two proteins (A , B) acting as transcription factors. Under certain conditions, this type of genetic network can show multistability. Here all possible regulatory modes are shown (+/-). In (b) a simplified diagram summarizes the logic of the system.

In a recent study (Guantes and Poyatos (2008)) on multistable circuits, the authors found tristable ($N = 3$) dynamics in genetic circuits of two components involving dimeric regulators. The computational analysis involved a systematic (both deterministic and stochastic) exploration of mutual-activation and mutual-inhibition circuits, i.e. circuits where the cross-regulatory inputs have the same sign. The study revealed very interesting properties of the resulting molecular switches, with relevant implications for cell behavioural patterns, It would be desirable to extend this approach to completely general scenarios, finding the mathematical conditions for different multistable patterns and how are they affected by the degree of multimerization. In this work we will focus our attention on the analysis of such a general, minimal genetic circuit and its potential multistable patterns. We use a systematic methodology to analytically establish possible types of dynamics displayed by two-component regulatory circuits. This method is based on the analysis of the crossings of nullclines, considering only simple, geometrical features. Specifically, for a two-dimensional dynamical system described by a pair of differential equations, namely:

$$\begin{aligned}\frac{dA}{dt} &= f(A, B) \\ \frac{dB}{dt} &= g(A, B)\end{aligned}\tag{1}$$

the nullclines are defined as the curves

$$\begin{aligned}f(A, B) &= 0 \\ g(A, B) &= 0\end{aligned}\tag{2}$$

or alternatively $\dot{A} = 0$ and $\dot{B} = 0$ (here \dot{x} indicates time derivation, i.e. dx/dt). The first (A-nullcline) curve corresponds to the points in the (A, B) phase plane where A does not change, whereas the second (B-nullcline) defines those where B is stable. The crossing points between both curves define the equilibrium points and the shape of the curves allows to identify their stability properties (Edelstein-Keshet (1988)).

Analyzing a minimal set of geometrical properties of the nullclines, allows to determine the necessary conditions for the emergence of mono- ($N = 1$), bi- ($N = 2$) or in general multistable ($N > 2$) dynamics. We show that two key ingredients are independently determinant for the mode of decision-making, namely the presence of an auto-regulatory feedback and the multimerization of the regulatory factors. Finally we present a numerical exploration of the feasibility of different types of dynamics and their robustness against parameter changes implemented by simple two-gene circuits. Our study shows that bistability is by far the dominant type of behaviour displayed by two component circuits.

Understanding these minimal systems sets the stage for the comprehension of more complex decision-making mechanisms present in nature (Kaufman and Thomas (2003); Ninfa and Mayo (2004)) and allows for sophisticated synthetic designs with biomedical applications. This knowledge, their logic and how it will change under parameter tuning are important goals of systems biology.

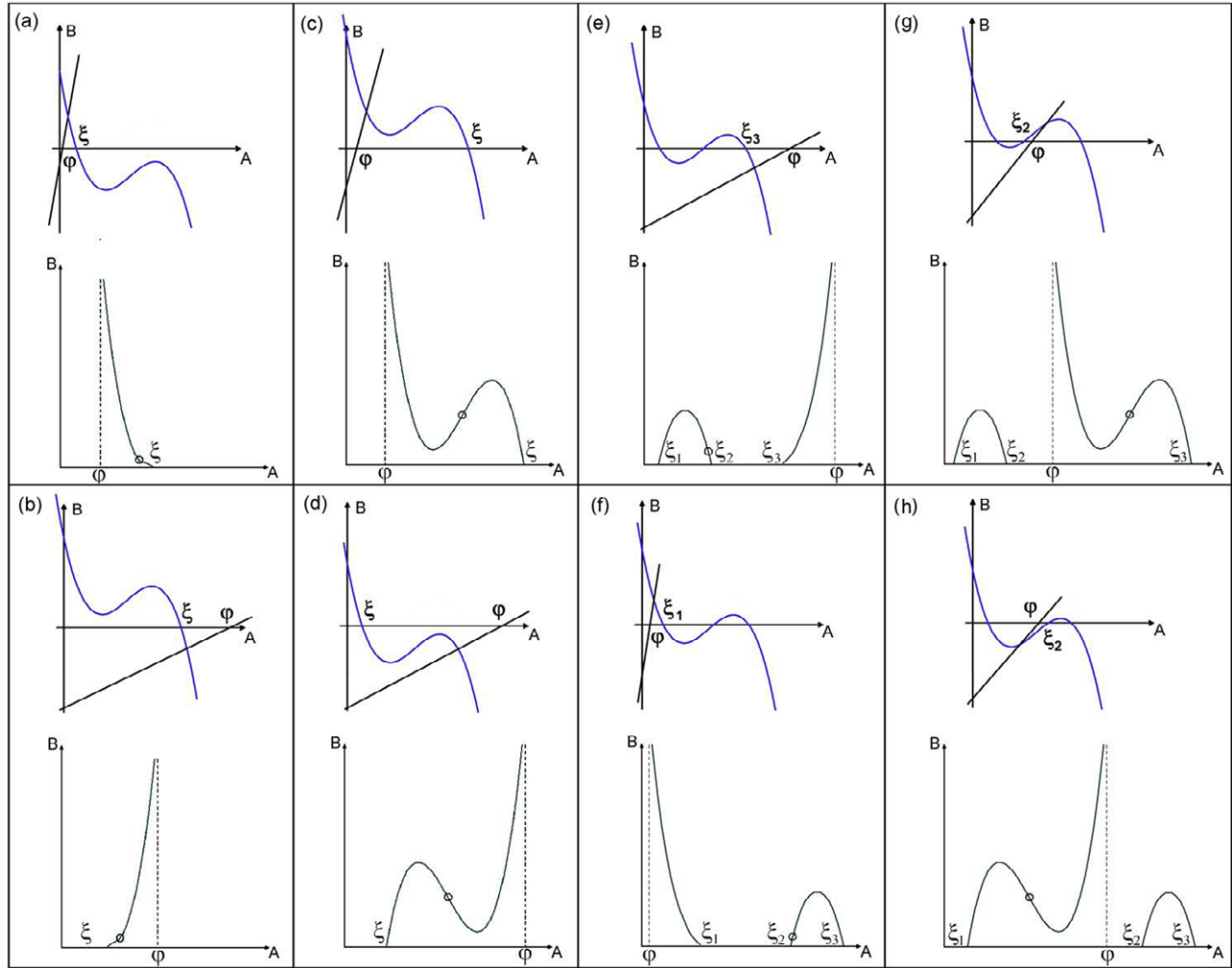


Figure 2: The possible qualitative geometries of the nullclines (bottom) deduced from the various combinations of numerator and denominator (top) considering only the biologically meaningful region, i.e. ($A > 0, B > 0$). Detailed example of the procedure is featured in the Appendix. The location of the vertical asymptote is denoted by φ and ξ_i indicates the crossing with the horizontal axis. The inflection point (open circle) and extrema, if exist, arise at the indicated locations, but not elsewhere.

2. Description of the genetic circuit

The analytic approach taken here considers the most general system formed by two genes. We consider a competitive model with a single binding site per gene, involving a minimal set of interactions. The qualitative properties found in this setting can be found in more complex models (considering e.g. cooperative regulation) as well. Expression of gene A is regulated by two different modes: firstly, protein A exhibits an auto-regulatory loop by binding to its own promoter; secondly, expression is cross-regulated by protein B. Gene B is regulated homologously (see figure 1).

The tunable parameters α_l^i and α_c^i describe the type of regulatory interactions, i.e. activation or inhibition, without any predefined specific assumptions. They denote the regulatory rates with respect to the basal transcription, for the autoloop and cross-regulation respectively. Parameter values smaller than one correspond to inhibitory regulation, whereas those larger account for activation. Modelling deterministically this two-component system on assuming basal transcription, the standard rapid equilibrium approximations and constant number of promoter sites, we obtain:

$$\dot{A} = \gamma_A \left(\frac{1 + \omega_l^A \alpha_l^A A^{n_l} + \omega_c^B \alpha_c^B B^{m_c}}{1 + \omega_l^A A^{n_l} + \omega_c^B B^{m_c}} \right) - d_A A \quad (3)$$

$$\dot{B} = \gamma_B \left(\frac{1 + \omega_l^B \alpha_l^B B^{m_l} + \omega_c^A \alpha_c^A A^{n_c}}{1 + \omega_l^B B^{m_l} + \omega_c^A A^{n_c}} \right) - d_B B \quad (4)$$

Here, the binding equilibrium of the autoloop and the cross-regulators are denoted by ω_l^i and ω_c^i , respectively. The degradation rate of protein i is denoted as d_i . The degree of multimerization of autoloop (l) and cross-regulators (c) is given by $n_{l,c}$ and $m_{l,c}$ for the respective proteins. Finally,

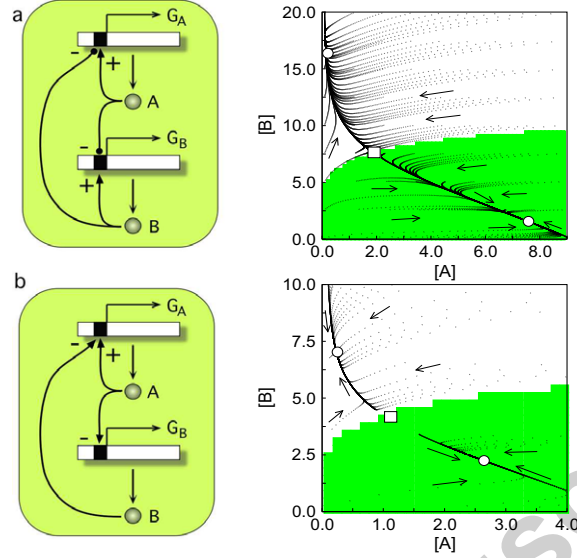


Figure 3: Numerical simulations and stability analysis of monomeric systems with (a) two and (b) one autoloop. Circle denotes a stable foci whereas white square denotes a saddle point. The basins of attraction are shown in green and white. The following sets of parameters have been used: (a) $\gamma_A = 1$, $d_A = 1$, $\alpha_l^A = 10$, $\omega_l^A = 1$, $\omega_c^B = 1$, $\alpha_c^B = 0$, $\gamma_B = 1.1$, $d_B = 0.1$, $\alpha_l^B = 2.1$, $\omega_l^B = 0.1$, $\omega_c^A = 1.1$, $\alpha_c^A = 0$ and (b) $\gamma_A = 5$, $d_A = 8$, $\alpha_l^A = 9$, $\omega_l^A = 1$, $\omega_c^B = 1$, $\alpha_c^B = 0$, $\gamma_B = 8.5$, $d_B = 1$, $\alpha_l^B = 0$, $\omega_l^B = 0$, $\omega_c^A = 1$, $\alpha_c^A = 0$

the concentration of other biochemical elements involved remain constant during time and can be subsumed in the kinetic constant γ_i .

3. Nullclines analysis

In order to analyze the system's dynamics we obtain the following expressions for the nullclines (i.e. imposing $\dot{A} = 0$ and $\dot{B} = 0$):

$$(B)_{\dot{A}=0} = \left(\frac{\gamma_A + \gamma_A \omega_l^A \alpha_l^A A^{\omega_l^A} - d_A A - d_A \omega_l^A A^{\omega_l^A + 1}}{\omega_c^B (d_A A - \gamma_A \alpha_c^B)} \right)^{\frac{1}{m_c}} \quad (5)$$

$$(A)_{\dot{B}=0} = \left(\frac{\gamma_B + \gamma_B \omega_l^B \alpha_l^B B^{m_l} - d_B B - d_B \omega_l^B B^{m_l+1}}{\omega_c^A (d_B B - \gamma_B \alpha_c^A)} \right)^{\frac{1}{n_c}} \quad (6)$$

The number of crossing points between (5) and (6) defines the number of different fixed points within the system. Both nullclines have symmetric expressions. This symmetry facilitates their analysis due to interchangeability of their characteristic features under exchange between variables A and B . Hence, the problem can be evaluated by focusing only on expression (5).

3.1. Geometric features

The qualitative shape of the nullclines and the resulting dynamical constraints are addressed by the analysis of a specific set of simple geometrical features, namely: the behaviour of the asymptotes, the crossing points with the axes, the extrema and the inflection points. First we will consider the geometrical features of the numerator and the denominator of the nullcline separately.

The denominator is a straight line independent of the degree of multimerization crossing the horizontal axis at

$$\varphi = \frac{\gamma_A \alpha_c^B}{d_A} \quad (7)$$

which determines the location of the vertical asymptote of the corresponding nullcline. The numerator is a polynomial of degree $n_l + 1$.

To determine the geometric features of the numerator we consider the crossing point of the numerator with the vertical axis in $B = \gamma_A$ and the number of crossing points ξ_i with the horizontal axis. The number of these points depends on the specific set of parameters, but are constrained between

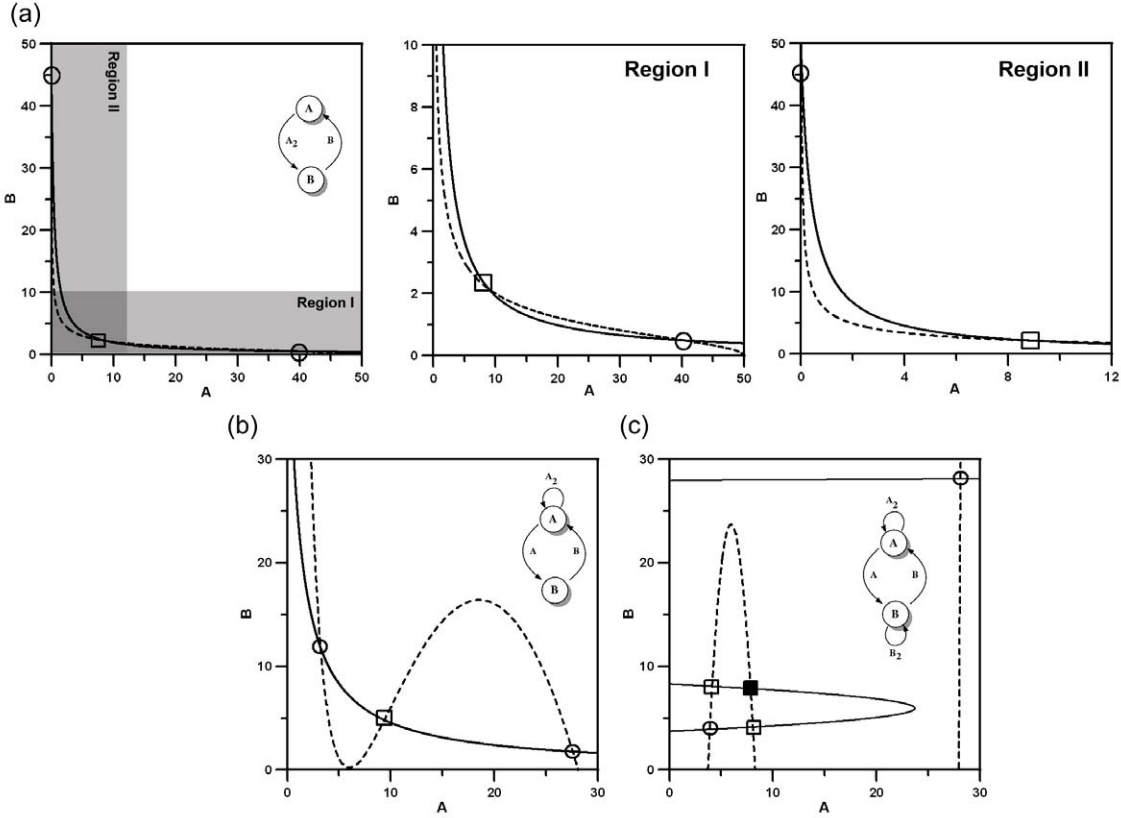


Figure 4: The minimal geometrical conditions implementing bistability, classified by the number of autoloops and the emergence of respective extrema. We show cases without (a) and with (b, c) extrema. The insets depict the topology of the genetic circuit. (a) Nullclines with $n_l = 0, m_c = 1$ and $m_l = 0, n_c = 2$ exhibiting an horizontal asymptote and an inflection point respectively with $\gamma_A = 5, d_A = 0.1, \alpha_l^A = 0, \omega_l^A = 0, \omega_c^B = 2.5, \alpha_c^B = 0, \gamma_B = 5, d_B = 0.1, \alpha_l^B = 0, \omega_l^B = 0, \omega_c^A = 1, \alpha_c^A = 0$. Region I and Region II (grey areas) have been plotted with more detail. In (b) a system of $n_l = 2, m_c = 1$ and $m_l = 0, n_c = 2$ is shown exhibiting extrema in a single nullcline based on a single autoloop, applying $\gamma_A = 0.271, d_A = 0.1, \alpha_l^A = 14.767, \omega_l^A = 2.7 \cdot 10^{-3}, \omega_c^B = 1.25 \cdot 10^{-2}, \alpha_c^B = 1.73 \cdot 10^{-3}, \gamma_B = 5, d_B = 0.1, \alpha_l^B = 0, \omega_l^B = 0, \omega_c^A = 1, \alpha_c^A = 0$. (c) Nullclines with $n_l = 2, m_c = 1$ and $m_l = 2, n_c = 1, \gamma_A = 0.236, d_A = 0.1, \alpha_l^A = 16.96, \omega_l^A = 2.7 \cdot 10^{-3}, \omega_c^B = 2.7 \cdot 10^{-4}, \alpha_c^B = 22.99, \gamma_B = 0.236, d_B = 0.1, \alpha_l^B = 16.96, \omega_l^B = 2.7 \cdot 10^{-3}, \omega_c^A = 2.7 \cdot 10^{-4}, \alpha_c^A = 22.99$. Circles indicate stable foci, white squares denote saddle points and black square represents unstable foci.

one and three. If $A \rightarrow \infty$ the polynomial tends to $-\infty$, and the numerator necessarily crosses the horizontal axis, due to the fact that the numerator crosses the vertical axis at a positive value γ_A . Furthermore the numerator exhibits a single inflection point (IP) in the biological domain, i.e. $A > 0$ and $B > 0$ at

$$A_{IP} = \frac{(n_l - 1)\alpha_l^A \gamma_A}{(n_l + 1)d_A}. \quad (8)$$

From this result two possible scenarios are expected to occur: i) no extrema in the biological domain and hence only one crossing with the horizontal axis is possible (i.e. the previously discussed crossing), ii) the numerator exhibits two extrema (a minimum followed by a maximum) and multiple (up to three) crossings are possible.

The shape of the nullcline is defined by the possible overlaps between the numerator and the denominator. In figure 2 all possible qualitative overlaps are shown. For illustrative purposes we discuss a full set of examples to demonstrate the effects of the overlap on the shape of the nullcline in the Appendix. Subfigures 2(a) - (f) present some examples of the shapes of the nullcline. Subfigures 2(g) and (h) represent scenarios with very specific location of φ : g) $\xi_2 < \varphi < A_{IP}$ and for h) $A_{IP} < \varphi < \xi_2$. The role of the genetic cross-regulation is represented by the exponent $1/m_c$ in (5). The value of m_c does not have a qualitative effect onto the crossings, the extrema nor on the vertical asymptote within the biological domain. However it exerts influence on the curvature and the exact position of the inflection point of the nullcline.

In the specific case of monomeric regulation $n_l = m_c = 1$ another geomet-

rical element appears related with the presence of autoloops, i.e. the oblique asymptotes with a slope $-\omega_i^A/\omega_c^B$. As we will see later this asymptote is a requirement for bistability in monomeric circuits. Additionally, no extrema are possible, preventing multistability beyond degree two.

Considering these basic geometrical features of the nullclines we can already classify the studied systems into two blocks: systems with monomeric regulation are qualitatively different from systems with multimeric regulation, which are characterized by a high level of nonlinearity, increasing with the degree of multimerization. These differences have their logical counterparts in their multistable dynamic potentials.

4. Analysis of the different multistable scenarios

In this section, we are aiming to overlap both nullclines (equations (5) and (6)) in order to obtain the full system, its respective fixed points and its level of stability: mono-, bi-, tri- and tetrastability. Once the geometrical requirements are satisfied, the degree of multistability depends on the given set of parameters. The essential geometrical properties are linked to two biological functions, i.e. the existence of the autoloop and the degree of multimerization of the feedback, as well as of the cross-regulation.

4.1. Bistability ($N = 2$)

Considering the different size of the multimeric regulators and circuit topologies, there are different ways to achieve bistability. Genetic circuits of two components without autoloops cannot exhibit bistability with monomeric regulators as shown by (Cherry and Adler (2000)). The biological mechanism

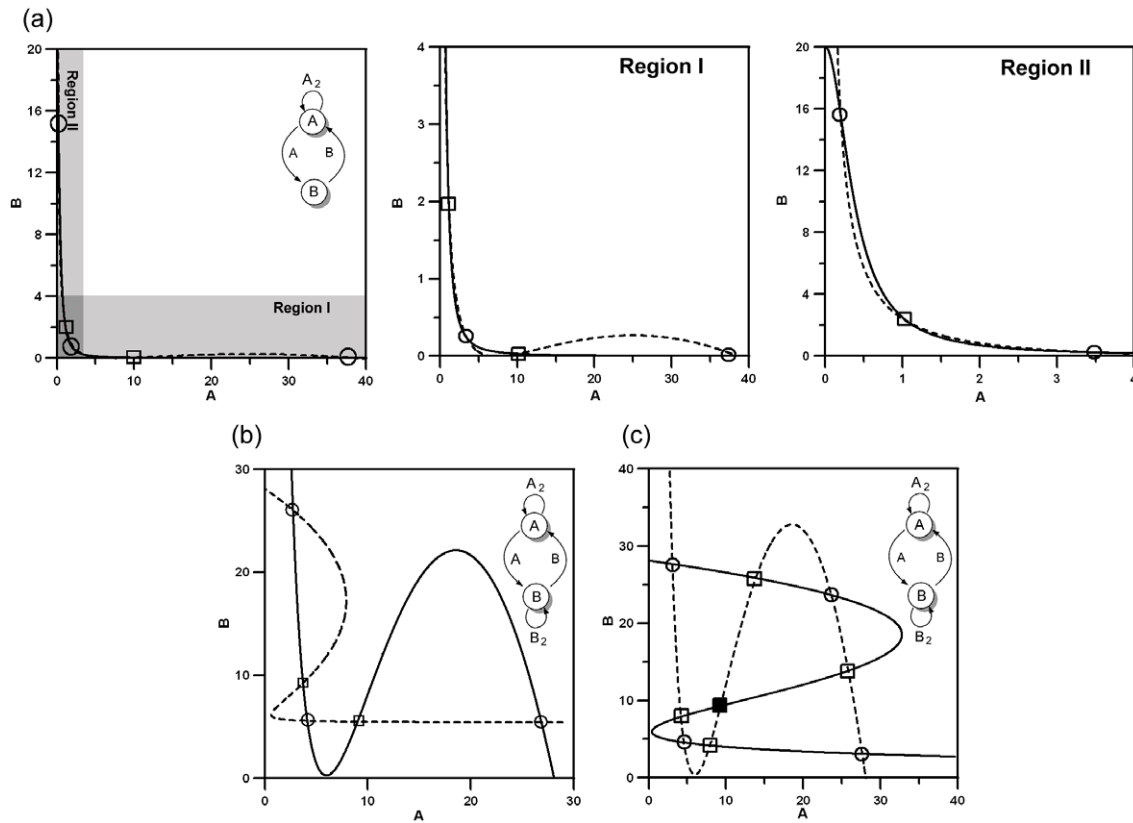


Figure 5: Examples of tri- (a, b) and tetrastable (c) systems. The minimal requirement for tristability is the existence of one autoloop as seen in (a). In (a) Regions I and II have been plotted in detail. For the emergence of tetrastability two autoloops are needed, as depicted in (c). Figure (a) Nullcline showing tristability for $n_l = 2$, $m_c = 1$ and $m_l = 0$, $n_c = 2$ with parameters $\gamma_A = 0.2$, $d_A = 6 \cdot 10^{-2}$, $\alpha_l^A = 16$, $\omega_l^A = 1.6 \cdot 10^{-3}$, $\omega_c^B = 1$, $\alpha_c^B = 0$, $\gamma_B = 2$, $d_B = 0.1$, $\alpha_l^B = 0$, $\omega_l^B = 0$, $\omega_c^A = 7$, $\alpha_c^A = 0$. (b) Tristability implemented by a circuit with two autoloops with parameters $n_l = 2$, $m_c = 1$ and $m_l = 2$, $n_c = 1$, respectively, $\gamma_A = 0.271$, $d_A = 0.1$, $\alpha_l^A = 14.767$, $\omega_l^A = 2.7 \cdot 10^{-3}$, $\omega_c^B = 1 \cdot 10^{-2}$, $\alpha_c^B = 1.73 \cdot 10^{-3}$, $\gamma_B = 0.271$, $d_B = 0.1$, $\alpha_l^B = 14.767$, $\omega_l^B = 2.7 \cdot 10^{-3}$, $\omega_c^A = 4 \cdot 10^{-2}$, $\alpha_c^A = 2$. The system (c) shows tetrastability based on inflection points and extrema in both nullclines $n_l = 2$, $m_c = 1$ and $m_l = 2$, $n_c = 1$, with the set of parameters $\gamma_A = 0.271$, $d_A = 0.1$, $\alpha_l^A = 14.767$, $\omega_l^A = 2.7 \cdot 10^{-3}$, $\omega_c^B = 6.75 \cdot 10^{-3}$, $\alpha_c^B = 1.73 \cdot 10^{-3}$, $\gamma_B = 0.271$, $d_B = 0.1$, $\alpha_l^B = 14.767$, $\omega_l^B = 2.7 \cdot 10^{-3}$, $\omega_c^A = 6.75 \cdot 10^{-3}$, $\alpha_c^A = 1.73 \cdot 10^{-3}$. Here circles denote stable foci, white squares saddle points and black square denotes unstable foci.

able to provide the minimal nonlinearity in the circuit response is the existence of a single monomeric autoloop. The existence of the autoloops allows for the presence of an oblique asymptote in the nullclines plot, which in turn provides the possibility to generate a bistable scenario (Wolf and Eeckman (1998)) as can be seen in figure 3. On the other hand, multimeric circuits without autoloops are able to provide bistability, but involving some geometrical differences. Now the oblique asymptote disappears and is substituted by the emergence of inflection points in the nullclines within the region $A > 0$ and $B > 0$. The size of the regulator has a direct effect in the position of the inflection points and increases the curvature of the nullclines at both sides of the inflection point. This development enhances the feasibility to encounter bistability. Finally the last qualitative scenario providing bistability involves multimeric circuits with autoloops, providing the degree of nonlinearity to introduce additional extrema to the nullclines. The extrema supply the circuits with a maximum of geometrical plasticity. In figure 4 we show the minimal biological requirements (in terms of circuit architecture and degree of multimerization) to obtain bistability via the different geometrical features described above.

More complex overlaps between nullclines with multiple geometrical elements can be considered, thus providing a huge amount of possible combinations for the emergence of bistability. Yet no new geometrical elements are involved.

4.2. *Tristability* ($N = 3$):

According with Poincare-Hopf theorem Glass (1975), in order to ob-

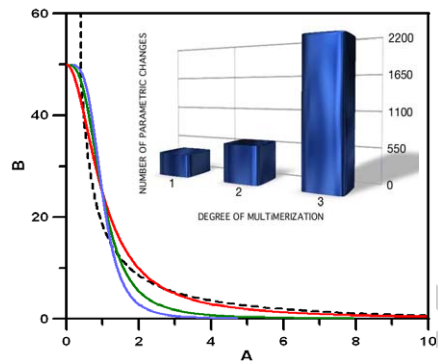


Figure 6: Effects of multimerization of the regulators on the geometry of the nullclines. With bigger regulator size, curvature increases enhancing the plasticity of the genetic circuit. The picture shows the nullclines of a minimal bistable circuit without autoloops. Regulator A is kept constantly monomeric (dashed line), whereas the size of regulator B is increased stepwise from di- (red), over tri- (green) to tetramers (blue). The increasing curvature is related with an increase in the robustness of the circuit against parametric changes. The inset (blue bars) shows the mean number of mutations needed to fall into the monostable regime. The simulations have been performed starting from the same set of parameters, changing only the size of the multimeric regulator.

tain tristability in a deterministic setting at least five nullcline crossings are needed. Three of the fixed points correspond to the stable states, while the other two provide the limits of the basins of attraction. Applying the previously described procedure, several combinations of differently shaped nullclines are feasible, providing tristable dynamics. All of them need to exhibit extrema in at least one of the nullclines, hence at least one multimeric autoloop is required. Figure 5 gives some examples of tristable systems for different circuits. In particular, in figure 5(a) we show an example of the least complex system allowing tristability, implemented by the reassembly of nullclines with $n_l = 2$, $m_c = 1$ and $m_l = 0$, $n_c = 2$. In figure 5(b) an example for a higher degree of complexity is shown. Ignoring the constraint of minimal interactions, further combinatorial scenarios exist comprising tristable dynamics.

4.3. *Tetrastability ($N = 4$):*

For the emergence of tetrastable behaviour, we need four stable fixed points. Due to the shape of our nullclines the only solution able to provide this number of stable fixed points involves the existence of five unstable fixed points as figure 5(c) shows. Under the geometrical point of view, this scenario is feasible only if both nullclines exhibit extrema. To satisfy the minimal geometrical requirements, the existence of two autoloops with multimeric regulators for both genes is necessary independently of the degree of multimerization of the cross-regulation.

4.4. *Beyond Tetrastability ($N > 4$):*

Systems with multimeric auto-regulation and nullcline shape of the type

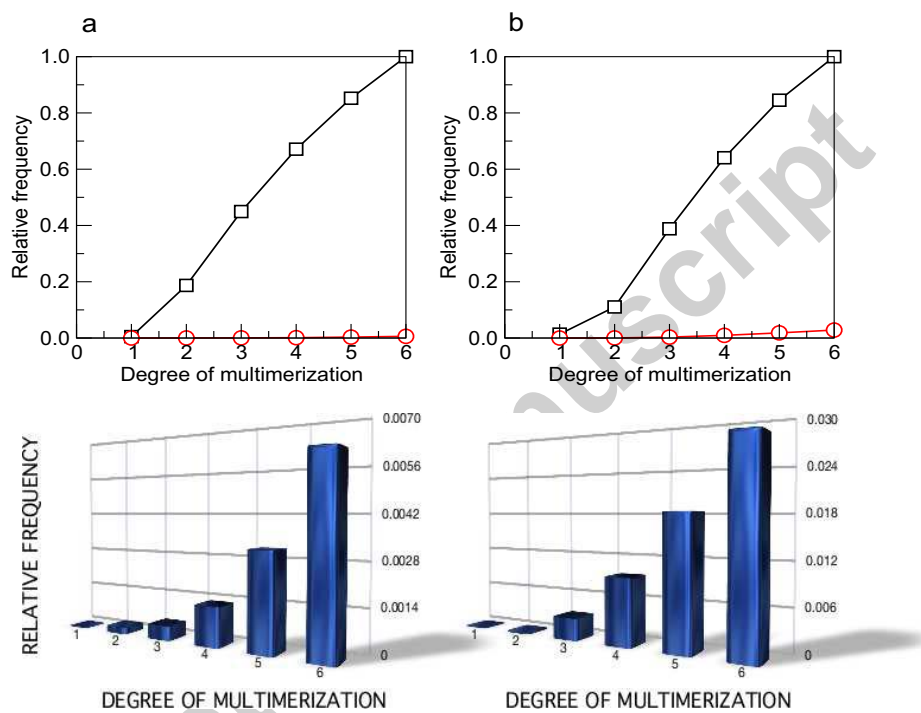


Figure 7: Relative frequency of parameter sets showing bistable (square), multistable (circle) behaviour. (a) Results for competitive regulation, (b) for cooperative regulation are shown. In both cases bistability is largely dominant. The relative frequency for non-bistable systems is higher in the cooperative model (blue bars shown below respectively).

shown in figure 2(g) and (h) can exhibit multistability beyond degree four. The maximally possible fixed points achieved by these scenarios can provide heptastability. However, these types of shape suffer from strong geometrical constraints, i.e. the numerator of the nullcline must exhibit three crossing with the horizontal axis and the denominator has to cross the horizontal axis within a very specific range located between the inflection point of the numerator and the second crossing of the numerator with the horizontal axis. This degree of multistability is exceptionally difficult to achieve, hence can probably not be implemented by this sort of circuit. Discarding these marginal scenarios the maximal degree of multistability achieved by these circuits is four.

5. Abundance and Robustness:

The geometrical analysis of the nullclines has shown that the case for strictly monomeric circuits is restricted to a single scenario, which can provide bistability at most. On the other hand, for dimeric or higher regulators we find more possible geometrical scenarios implementing multistability. These scenarios stay qualitatively identical independently of the degree of multimerization.

A priori this fact suggests that the biggest qualitative difference lies in the transition between monomeric and multimeric regulation. However, the increase of the size of the multimeric regulators has a relevant effect in the feasibility of the scenarios implementing multistability, since along with multimerization level there is an increase in the curvature of the nullclines and

the centering of the inflection point within the region $A > 0$ and $B > 0$. These effects provide easier access to a higher number of crossing points. The same argument holds for robustness versus parameter change. Numerical simulations have shown that the mean number of parametric mutations required to lose bistable behaviour increases with multimer size. This indicates that bistable systems with higher multimerization degree are more robust versus parametric change. Figure 6 shows some illustrative examples.

To understand in detail the role of the regulator size, we performed a numerical study calculating the abundance of bistability versus multistability in parameter space. We assume that each possibly implemented dynamic has an associated parameter space, in which the respective type of dynamic is realised. The conjecture is that dynamics with a larger parameter space will be encountered more abundantly. We are choosing random sets of parameters in a wide range for the equations (3) and are analyzing the dynamics of the system in terms of bistability and multistability (three or more stable states). We have found that for all circuits under investigation, bistability is largely dominant over multistability as shown in figure 7. The same analysis has been performed for circuits with cooperative binding and similar qualitative results have been obtained. That suggest, that even though various types of dynamics can be implemented by two-gene networks, these circuits are optimal to implement Boolean switches.

By increasing the size of the regulators, it is possible in principle to enhance the absolute frequency of appearance of multistable parameter sets.

However, the ratio between bistable systems and the rest remains practically constant. These numerical results are consistent with the fact that the geometrical constraints defining each scenario increase with the number of stable states. In other words, the number of viable biological scenarios able to provide a given type of multistability, decreases. From the presented results we assume that circuits efficient implementing multistable behaviour should involve either a more complex topology or larger, heteromeric regulator complexes.

6. Conclusions

Regulatory networks define the computational machinery of life at the cellular level. They largely define the cell hardware, allowing cells to preserve or change their internal state, adapt to changing conditions or even die. Most of these events result from the presence of molecular switches. Bistability, catastrophes and hysteresis have been identified as key dynamical phenomena pervading such switching behavior (Tyson et al. (2008)). Many complex processes taking place at different levels are strongly tied to such switch-like decisions. Waddington's picture of developmental paths, would be an example of this ideas (Waddington (1957)). As the embryo grows and changes its shape, cells undergo switching transitions, with different genes turning ON or OFF as a result of both intra- and cell-cell interactions (Kauffman (1993); Forgacs and Newman (2005)). In many cases, the resulting spatial patterns can be explained in terms of simple regulatory modules (Sole et al. (2002))

Although there is a large literature devoted to multistability in high-dimensional dynamical systems and a few low-dimensional cases (Mendoza

and Alvarez-Buylla (2000); Glass and Kauffman (1973); Snoussi and Thomas (1993)) many relevant questions remain open. In this paper, the general problem of the possible and the actual two-component circuits has been analytically (and numerically) addressed, focusing on the feasibility of occurrence of bi- or higher order multistability. The results obtained so far allow to reach two basic conclusions.

We have shown that tri- and tetra-stability are also possible outcomes of simple, two-component regulatory networks. Our analysis allows to predict the set of conditions under which such multiple states are expected to occur. The emergence of different dynamics is closely related to the circuit topology (i.e. number of autoloops) as well as the degree of multimerization of the regulators. We have seen that there exists a great qualitative difference between strictly monomeric circuits and circuits involving multimeric regulators. Monomeric, competitive circuits are able to provide at most bistability, whereas networks involving multimers can achieve at most tetrastability independently of the specific size of the regulator. In order to obtain bistability no special topological requirement, in terms of autoloops, must be met. However, the necessary geometrical constraints for tri- and tetrastability impose the existence of at least one or two multimeric autoloops, respectively. The degree of multimerization, however, plays an important role in the frequency of emergence and the robustness versus parametric changes of the different multistable dynamics. Increasing the size of the multimer implies an increase of frequency and robustness.

Are multistable solutions equally likely to be implemented by two-gene

networks in molecular systems? Although only a few have been reported so far, they are possible and thus, should be designable using synthetic biology techniques. However, our results indicate that despite that simple two-gene circuits are able to implement a variety of different multistable behaviour, their optimal regime is bistability. This is consistent with the scarcity of biological two-gene circuits which have been reported to implement multistability so far. Our study shows that the size of bistable parameter space is dominantly larger than any other alternative dynamic spaces. We suspect that the rarity of multistable dynamics in two-component regulatory circuits might be explained from our analysis and that the number of constraints required to reach a genetic switch with more than two stable states using only two regulatory elements, might be too large for natural selection to find it. Future work is required to determine the optimal topological and regulatory configuration to implement multistable decision processes.

7. ACKNOWLEDGMENTS

We thank the members of the CSL for useful discussions. This work was supported by the EU grant CELLCOMPUT, the EU 6th Framework project SYNLET (NEST 043312), the James McDonnell Foundation and by the Santa Fe Institute.

References

Abramowitz, M., Stegun, I. A. (Eds.), 1964. Handbook of mathematical functions with formulas, graphs and mathematical tables. NBS Applied Mathematics Series 55. National Bureau of Standards, Washington, DC.

- Boyer, L., Lee, T. I., Cole, M. F., Johnstone, S. E., Levine, S. S., Zucker, J. P., Guenther, M. G., Kumar, R. M., Murray, H. L., Jenner, R. G., Gifford, D. K., Melton, D. A., Jaenisch, R., Young, R. A., 2005. Core transcriptional regulatory circuitry in human embryonic stem cells. *Cell* 122, 947–56.
- Cantor, A. B., Orkin, S. H., 2001. Hematopoietic development: a balancing act. *Curr. Opin. Genet. Dev.* 11, 513–9.
- Cherry, J. L., Adler, F. R., 2000. How to make a biological switch. *J. Theor. Biol.* 203, 117–133.
- Chickarmane, V., Troein, C., Nuber, U. A., Sauro, H. M., Peterson, C., 2006. Transcriptional dynamics of the embryonic stem cell switch. *PLOS Comput. Biol.* 2, 1080–1092.
- Cinquin, O., Demongeot, J., 2005. High-dimensional switches and the modelling of cellular differentiation. *J. Theor. Biol.* 233, 391–411.
- Delbrück, M., 1949. Discussion in 'Unités biologiques douées de continuité génétique'. *Colloq. Int. CNRS* 8, 3335.
- Demongeot, J., Kaufman, M., Thomas, R., 2000. Positive feedback circuits and memory. *C. R. Acad. Sci. III* 323, 69–79.
- Edelstein-Keshet, L., 1988. *Mathematical models in biology*. Birkhauser Mathematics Series. McGraw-Hill.
- Ferrell, J. E., Machleder, E. M., 1998. The biochemical basis of an all-or-none cell fate switch in *xenopus* oocytes. *Science* 280, 895–898.

- Forgacs, G., Newman, S., 2005. *Biological physics of the developing embryo*. Cambridge U. Press. Cambridge.
- Glass, L., 1975. A topological theorem for nonlinear dynamics in chemical and ecological networks. *Proc. Natl. Acad. Sci. USA* 75, 2856–2857.
- Glass, L., Kauffman, S. A., 1973. The logical analysis of continuous, nonlinear biochemical control networks. *J. Theor. Biol.* 39(1), 103–129.
- Guantes, R., Poyatos, J. F., 2008. Multistable decision switches for flexible control of epigenetic differentiation. *PLoS Comput. Biol.* 4, doi:10.1371/journal.pcbi.1000235.
- Hasty, J., Isaacs, F., Dolnik, M., McMillen, D., Collins, J., 2001. Designer gene networks: Towards fundamental cellular control. *Chaos* 11, 207–220.
- Kauffman, S., 1993. *Origins of the order*. Oxford Univ. Press. New York.
- Kaufman, M., Thomas, R., 1987. Model analysis of the bases of multistationarity in the humoral immune response. *J. Theor. Biol.* 129, 141–162.
- Kaufman, M., Thomas, R., 2003. Emergence of complex behaviour from simple circuit structures. *C. R. Biol.* 326, 205–214.
- Laurent, M., Kellershohn, N., 1999. Multistability: a major means of differentiation and evolution in biological systems. *Trends Biochem. Sci.* 24, 418–422.
- Li, E., 2002. Chromatin modification and epigenetic reprogramming in mammalian development. *Nat. Rev. Genet.* 3, 662–73.

- Ma, J., Wu, J., 2007. Multistability in spiking neuron models of delayed recurrent inhibitory loops. *Neural. Comput.* 19, 2124–2148.
- Mendoza, L., Alvarez-Buylla, E. R., 2000. in *arabidopsis thaliana: A network model*. *J. Theor. Biol.* 204, 311–326.
- Ninfa, A. J., Mayo, A. E., 2004. Hysteresis vs. graded response: The connections make all the difference. *Science* 232, pe20.
- Niwa, H., Toyooka, Y., Shimosato, D., Strumpf, D., Takahashi, K., Yagi, R., Rossant, J., 2005. Interaction between Oct3/4 and Cdx2 determines trophectoderm differentiation. *Cell* 123, 142–7.
- Novak, B., Tyson, J. J., 2003. Modelling the controls of the eukaryotic cell cycle. *Biochem. Soc. Trans.* 31, 1526–9.
- Ozbudak, E. M., Thattai, M., Lim, H. N., Shraiman, B. I., Oudenaarden, A. V., 2004. Multistability in the lactose utilization network of *escherichia coli*. *Nature* 427, 737–40.
- Pomerening, J. R., Sontag, E. D., Ferrell, J. E., 2003. Building a cell cycle oscillator: hysteresis and bistability in the activation of Cdc2. *Nat. Cell. Biol.* 5, 346–351.
- Snoussi, E., Thomas, R., 1993. Logical identification of all steady states: The concept of feedback loop characteristic states. *Bull. Math. Biol.* 55(5), 973–991.
- Sole, R. V., Salazar-Ciudad, I., Garcia-Fernandez, J., 2002. Common pattern

formation, modularity and phase transitions in a gene network model of morphogenesis. *Physica A* 305, 640–647.

Tyson, J., Albert, R., Goldbeter, A., Ruoff, P., Sible, J., 2008. Biological switches and clocks. *Journal of the Royal Society Interface. Special Supplement*. Vol. 5.

Tyson, J. J., Chen, K. C., Novak, B., 2003. Sniffers, buzzers, toggles and blinkers: dynamics of regulatory and signaling pathways in the cell. *Curr. Opin. Cell. Biol.* 15, 221–31.

Waddington, C., 1957. *The strategy of genes*. George Allen and Unwin. London.

Widder, S., Schicho, J., Schuster, P., 2007. Dynamic patterns of gene regulation I: simple two-gene systems. *J. Theor. Biol.* 246, 394–419.

Wolf, D. M., Eeckman, F. H., 1998. On the relationship between genomic regulatory element organization and gene regulatory dynamics. *J. Theor. Biol.* 195, 67–86.

Zhou, Q., Chipperfield, H., Melton, D. A., Wong, W. H., 2007. A gene regulatory network in mouse embryonic stem cells. *Proc. Natl. Acad. Sci. U S A* 104, 16438–43.

8. Appendix

In order to describe the procedure for the determination of the nullcline's shape we present some examples in detail.

Starting from the nullcline expressions (5) and (6), we independently analyze the behaviour of the numerator and the denominator, which puts us into the position to discern possible combinatorial scenarios of interplay between the two parts of the expression. Subsequently we reassemble and study the geometric properties of the entire nullcline, before mounting the combinatorial of the whole system, represented by both nullclines. The deduction of the relevant geometrical properties of the nullcline follows the standard procedure (Abramowitz and Stegun (1964)). Here, we are focusing on the cases with monomeric cross-regulation $m_c = 1$. The cases of dimeric cross-regulation, $m_c = 2$, have the same geometrical features as their monomeric counterparts, except the number of inflection points, which is usually higher.

The number of extrema of the nullcline is a significant factor in the emergence of multistability. The biological mechanism behind the existence of extrema is the auto-regulation. Due to the fact that the degree of the nullcline's expression increases with the degree of multimerization, in principle multiple extrema are possible. However, the fact that the numerator can only exhibit a single inflection point within the biological domain and hence only two extrema, constraints the number of total extrema of the nullcline within the biological region to maximal three (see figure (8)).

The different shapes of the nullcline can be classified based on two elements: i) number of solutions for the crossings between the nullcline and the horizontal axis ξ_i , namely, a single or more crossings and ii) the position of the

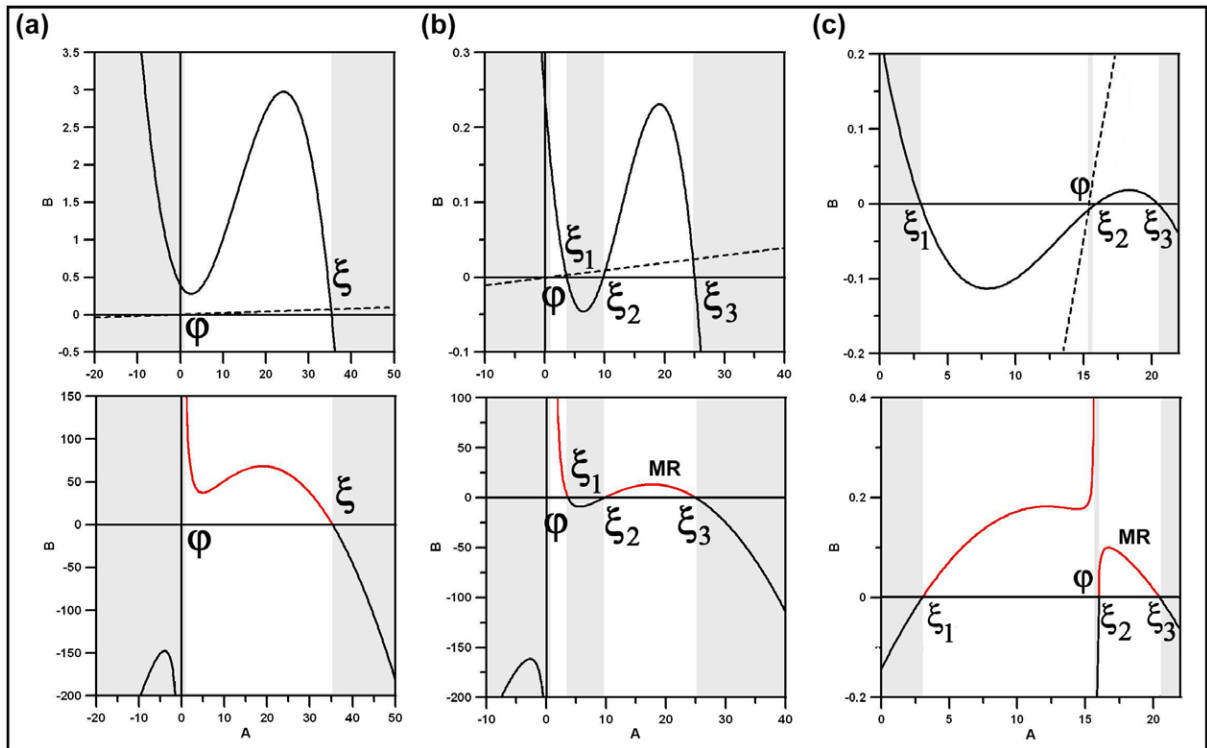


Figure 8: The shape of the nullclines $n_l = 2$, $m_c = 1$ (lower panel) deduced from the overlap of numerator and denominator (upper panel). The upper picture is the representation of the numerator (solid line) and the denominator (dashed line) independently. The lower picture shows the corresponding nullclines within the entire mathematical domain. In red we depict the biologically feasible region ($B > 0$, $A > 0$). The grey regions indicate the negative part of the nullclines ($B < 0$). The limits of the grey zones correspond to the different crossings of the numerator (ξ_i) and the denominator (φ) with the horizontal axis. For the nullclines with only two crossings with the horizontal axis (not shown), the distance between the asymptotically dominated region and the MR collapses into a minimum of the nullcline, without any further qualitative effects on its shape. Systems with $m_c = 2$ display qualitatively similar properties within the positive region, however, the negative region does not exist for \mathbb{R} and a higher number of inflection points are possible. The parameters are as follows: (a) $\gamma_A = 0.4$, $d_A = 0.1$, $\alpha_l^A = 10$, $\omega_l^A = 5.4 \cdot 10^{-3}$, $\omega_c^B = 2 \cdot 10^{-2}$, $\alpha_c^B = 0$, (b) $\gamma_A = 0.24$, $d_A = 0.1$, $\alpha_l^A = 16$, $\omega_l^A = 2.7 \cdot 10^{-3}$, $\omega_c^B = 1 \cdot 10^{-2}$, $\alpha_c^B = 0.4$, (c) $\gamma_A = 0.225$, $d_A = 0.1$, $\alpha_l^A = 17.5$, $\omega_l^A = 2.3 \cdot 10^{-3}$, $\omega_c^B = 1$, $\alpha_c^B = 7$.

vertical asymptote located at the abscissa $\varphi = \gamma_A \alpha_c^B / d_A$. For example, considering a single crossing, two possible scenarios can emerge i) $\varphi < \xi$ (figure (8)a) and ii) $\xi < \varphi$ resulting in qualitatively equal behaviour of the nullcline, but mirrored across the vertical asymptote.

Considering three crossings, again two different geometries emerge i) $\varphi < \xi_1 \vee \varphi > \xi_3$ and ii) $\xi_1 < \varphi < \xi_3$. The biological branch of the nullcline is split into two parts at varying distance, the asymptotic and the *MR* region, respectively. Under the first condition and in $B > 0$ the asymptotic region does not exhibit extrema, whereas *MR* accommodates a single maximum (see figure 8(b)). Under the second condition the extrema might be accommodated differently. Of the maximally three extrema, one is again used by *MR*, whereas the other two can locate to the asymptotic region lateral to an inflection point (figure 8(c)).

More different geometrical combinations of numerator and denominator are possible, see figure 2.